Applied Clay Science 100 (2014) 60–65

Contents lists available at ScienceDirect

Applied Clay Science

journal homepage: www.elsevier.com/locate/clay

Research paper

High-capacity loading of 5-fluorouracil on the methoxy-modified kaolinite

Daoyong Tan [a,b], Peng Yuan [a,*], Faïza Annabi-Bergaya [c], Dong Liu [a], Hongping He [a]

[a] CAS Key Laboratory of Mineralogy and Metallogeny, Guangzhou Institute of Geochemistry, Chinese Academy of Sciences, Guangzhou 510640, China
[b] University of the Chinese Academy of Sciences, Beijing 100039, China
[c] Centre de Recherche sur la Matière Divisée, CNRS-Université d'Orléans, Orléans 45071, France

ARTICLE INFO

Article history:
Received 17 October 2013
Received in revised form 20 February 2014
Accepted 22 February 2014
Available online 14 March 2014

Keywords:
Kaolinite
5-Fluorouracil
Methoxy modification
Intercalation

ABSTRACT

Kaolinite and methoxy-modified kaolinite were used as carriers for the loading of 5-fluorouracil (5FU) for the first time. The kaolinite products were characterized using X-ray diffraction, transmission electron microscopy, elemental analysis, diffuse reflectance infrared Fourier transform spectroscopy, thermogravimetric analysis, and differential scanning calorimetry. The loading mechanism of 5FU on kaolinite was as follows: the 5FU molecules were initially anchored to the external surface of kaolinite through hydrogen bonding, and the added 5FU then formed hydrogen-bonded aggregates with the anchored 5FU on the external surface of kaolinite. The surface-loaded 5FU was crystallite. The 5FU-loading content in the methoxy-modified kaolinite was 55.4 mass%, which was 147.3% greater than that in unmodified kaolinite. The high-capacity loading of 5FU on methoxy-modified kaolinite resulted from two factors: (i) the interlayer space of the methoxy-modified kaolinite acted as an additional loading site that was available for the intercalation of 5FU; (ii) the loading of 5FU on the external surface of the methoxy-modified kaolinite was high because of the high affinity between 5FU and the methoxy-modified kaolinite. The 5FU-loading content of the interlayer-loaded 5FU and the surface-loaded 5FU in the methoxy-modified kaolinite was 14.6 mass% and 40.8 mass%, respectively. The interlayer-loaded 5FU was in an amorphous state, and of higher thermal stability than the surface-loaded 5FU. Methoxy-modified kaolinite is a promising drug carrier in pharmaceutical industry.

1. Introduction

Naturally occurring clay minerals have been used widely as active pharmaceutical ingredients and excipients in the pharmaceutical industry because of their excellent rheological properties and inert chemical properties, as well as their low or null toxicity (Carretero, 2002; Carretero and Pozo, 2009, 2010). Clay minerals have also attracted great interest as drug carriers. Generally, the loading of drugs onto the clay minerals is achieved *via* two routes: (i) intercalation through ion exchange into the interlayer space of swelling clay minerals with a large cation/anion exchange capacity, such as montmorillonite, saponite, and layered double hydroxides (Akalin et al., 2007; Choy et al., 2007; Lin et al., 2002; Wang et al., 2005); and (ii) encapsulation into the inner nanopores and/or adsorption onto the external surface of clay minerals with a high specific surface area, such as halloysite (Lvov et al., 2008; Price et al., 2001; Tan et al., 2013; Yuan et al., 2008, 2012).

Kaolinite is a 1:1 clay mineral consisting of $AlO_2(OH)_4$ octahedral sheet and SiO_4 tetrahedral sheet. The adjacent sheets are connected together by the plane of apical oxygen of tetrahedral SiO_4 sheet to form a kaolinite layer with ideal chemical formula $Al_2Si_2O_5(OH)_4$. The kaolinite layers are joined by hydrogen bonding. Kaolinite is often used as an active pharmaceutical ingredient and excipient in pharmaceutics (Carretero and Pozo, 2009, 2010). Due to the low cation exchange capacity (always lower than 10 mmol/100 g) (Ma and Eggleton, 1999) and the low specific surface area of kaolinite (approximately 10 to 20 m^2/g) (Castellano et al., 2010), the drugs only adsorbed onto the external surfaces (Bonina et al., 2007; Mallick et al., 2008), and did not intercalate into the hydrogen-bonded interlayer. This drawback of a low kaolinite loading capacity, has severely limited the application of kaolinite as a drug carrier in pharmaceutics.

The drug 5-fluorouracil ($C_4H_3FN_2O_2$; 5FU) has been used extensively in cancer chemotherapy (including colon, rectum, and head and neck cancers) for over 40 years. The toxicity of 5FU may bring some adverse effects (including myelosuppression, mucositis, dermatitis, *etc.*) in humans. Embedding 5FU in a proper nanoparticle carrier can improve its anticancer activity and alleviate these adverse effects. The loading of 5FU in polymeric nanoparticles (McCarron et al., 2000; Niwa et al., 1993), zeolites (Datt et al., 2013), and some clay minerals, such as montmorillonite (Akalin et al., 2007; Lin et al., 2002), saponite (Akalin et al.,

* Corresponding author at: Guangzhou Institute of Geochemistry, Chinese Academy of Sciences, Wushan, Guangzhou 510640, China. Tel./fax: +86 20 85290341.
E-mail address: yuanpeng@gig.ac.cn (P. Yuan).

http://dx.doi.org/10.1016/j.clay.2014.02.022
0169-1317/

2007), and layered double hydroxides (Wang et al., 2005), has been reported. However, the loading of 5FU on kaolinite has not yet been reported.

In this work, the performance of kaolinite as a drug carrier for the loading of 5FU was studied for the first time. In particular, the effect of methoxy modification of kaolinite on the loading of 5FU was investigated. In previous studies, the methoxy-modified kaolinite has been used as a host to load some organic guests into the interlayer space through an intercalation route. The intercalated organic guests include ε-caprolactam (Komori et al., 1999a), poly(vinylpyrrolidone) (Komori et al., 1999b), alkylamines (Komori et al., 1999c), *p*-nitroaniline (Kuroda et al., 1999; Takenawa et al., 2001), nylon-6 (Matsumura et al., 2001), and some quaternary ammonium salts (Kuroda et al., 2011). However, the use of the interlayer space of the methoxy-modified kaolinite for the loading of drugs has not yet been explored.

2. Experimental section

2.1. Materials and methods

A kaolinite sample with high purity, obtained from Maoming Guangdong Province, China, was used as received without further purification. The chemical composition of kaolinite (SiO_2, 46.75; Al_2O_3, 39.15; Fe_2O_3, 1.02; MgO, 0.10; CaO, 0.21; K_2O, 0.25; Na_2O, 0.26; MnO, 0.01; TiO_2, 0.32; P_2O_5, 0.04; and loss on ignition, 11.92) was determined from the chemical analysis in percent by mass of the respective oxide forms.

The methoxy-modified kaolinite was prepared as follows: dimethyl sulfoxide (DMSO) was first intercalated into the interlayer space of the kaolinite as previously reported (Yang et al., 2012). Then, 5.0 g of the DMSO-intercalated kaolinite was added to 100 mL methanol (MeOH) and stirred for 7 days. The solid in the mixture was separated using centrifugation and stored in a wet state for further use. The methoxy-modified kaolinite was labeled as Kaol-MeOH.

The loading of 5FU was achieved using soaking methods. A sample of 0.5 g of 5FU (99%, purchased from Meryer) was dissolved in 20 mL of MeOH, and approximately 1.0 g of kaolinite (modified and unmodified) was added under constant stirring for 24 h at room temperature. The solid part of the dispersion was separated using centrifugation and dried overnight at 80 °C. The 5FU-loaded kaolinite samples were labeled as 5FU-Kaol-MeOH and 5FU-Kaol, corresponding to the Kaol-MeOH and kaolinite precursors, respectively.

2.2. Characterization methods

The X-ray diffraction (XRD) patterns were obtained using a Bruker D8 Advance diffractometer with a Ni filter and Cu Kα radiation ($\lambda = 0.154$ nm) generated at 40 kV and 40 mA. The scan rate was 1° (2θ) min^{-1} with a step size of 0.02°. The mean diameter of the 5FU crystallite loaded in kaolinite is evaluated using the Scherrer equation ($D = k\lambda/\beta\cos\theta$), where k is the shape factor with a value of 0.89, β is the integral breadth of the Bragg reflection, λ is the radiation wavelength applied and θ is the Bragg angle (Burton et al., 2009).

Diffuse reflectance infrared Fourier transform (DRIFT) spectra were obtained using a Bruker Vertex 70 Fourier transform infrared spectrometer at room temperature. All spectra were collected over 64 scans in the range of 4000 to 600 cm^{-1} at a resolution of 4 cm^{-1}.

The CHN elemental analyses were performed with an Elementar Vario EL III Universal CHNOS Elemental Analyzer. The 5FU content (M_{5FU}, g 5FU g^{-1} kaolinite) was calculated as $M_{5FU} = mass_N/N_{5FU}$, where N_{5FU} is the content of N in 5FU, and $mass_N$ the mass percentage of N in 5FU is determined from the CHN analysis.

Thermogravimetry (TG) and differential scanning calorimetry (DSC) analyses were performed with a Netzsch STA 409PC instrument. Approximately 10 mg of sample powder was heated in an Al_2O_3 crucible from 30 °C to 1000 °C at a rate of 10 °C/min under a highly pure N_2 atmosphere (60 cm^3/min).

Transmission electron microscopy (TEM) observations were conducted on a 200 kV JEOL JEM-2100 high-resolution transmission electron microscope. The specimens were prepared as follows: the 5FU loaded kaolinite was ultrasonically dispersed in water for 5 min, and then a drop of the dispersion was deposited onto a carbon-coated copper grid, which was left to stand for 10 min before being transferred into the microscope.

3. Results and discussion

3.1. XRD, TEM, and elemental analysis

Kaolinite shows a typical diffraction pattern with a characteristic d_{001} value of 0.71 nm (Fig. 1a). The wet Kaol-MeOH shows a (001) diffraction at 1.11 nm (Fig. 1b), indicating a monolayer intercalation of MeOH molecules in the interlayer space of kaolinite. The remaining reflection at 0.71 nm in Kaol-MeOH is due to the unintercalated kaolinite. The intercalation ratio of Kaol-MeOH is approximately 96.0%, as calculated from the equation:

$$IR = I_I/(I_K + I_I)$$

where I_K and I_I are the intensities of (001) diffractions of kaolinite and Kaol-MeOH, respectively (Lagaly et al., 2006).

The d_{001} value of 5FU-Kaol remains unchanged (Fig. 1c), indicating that 5FU did not intercalate into the interlayer spaces of kaolinite. This result is in agreement with that only small, polar organic compounds, such as dimethyl sulfoxide, methyl formamide, hydrazine, and urea, *etc.*, can be directly intercalated into the interlayer space of kaolinite by forming hydrogen bonds with the inner-surface hydroxyl groups (Frost et al., 1997, 1998, 2000).

The 5FU-Kaol-MeOH shows a (001) diffraction with an increased *d*-spacing of 1.27 nm (Fig. 1d), compared with the d_{001} value of 1.11 nm for Kaol-MeOH, indicating that the intercalation of 5FU in the interlayer space of the methoxy-modified kaolinite is achieved. This result shows that the methoxy modification makes the interlayer space of kaolinite available for 5FU loading. The molecular dimensions of 5FU are approximately 0.49 nm × 0.53 nm (Datt et al., 2013), and the d_{001} value of dry Kaol-MeOH is 0.82 nm (Komori et al., 2000; Tunney and Detellier, 1996), suggesting that 5FU might be arranged as a roughly vertical monolayer in the interlayer space of kaolinite (Fig. 1e). In the XRD pattern of 5FU-Kaol-MeOH, the broad and weak (001) reflection suggests a low structural order of the 5FU-intercalated kaolinite, and also implies a heterogeneous arrangement of 5FU in the interlayer space of kaolinite, which means several monolayer arrangements of 5FU with different inclination angles existed in the interlayer space of kaolinite. By using the stereochemical calculations based on molecular dynamics simulations, Zeng et al. (2003) also proposed that the actual configuration of the intercalated organic guests is much more complicated than the ideal configuration.

The reflection in the XRD pattern of 5FU-loaded kaolinite that corresponds to a *d* value of 0.31 nm can be assigned to 5FU according to reference No. 42-1969 of the Joint Committee on Powder Diffraction Standard in the International Centre for Diffraction Data database. This reflection is used for the calculation of the mean diameter (D) of 5FU crystallites by the Scherrer equation. The calculated D values of the 5FU crystallites in 5FU-Kaol and 5FU-Kaol-MeOH are 35.5 and 34.4 nm, respectively. Because the interlayer space of the methoxy-modified kaolinite was not large enough for the crystallization of 5FU (Sliwinska-Bartkowiak et al., 2001), the intercalated 5FU was in an amorphous state. This situation is similar to the intercalation of 5FU into the montmorillonite and layered double hydroxides (Lin et al., 2002; Wang et al., 2005) where 5FU did not crystallize in the confined interlayer space of the clay minerals and formed in the amorphous

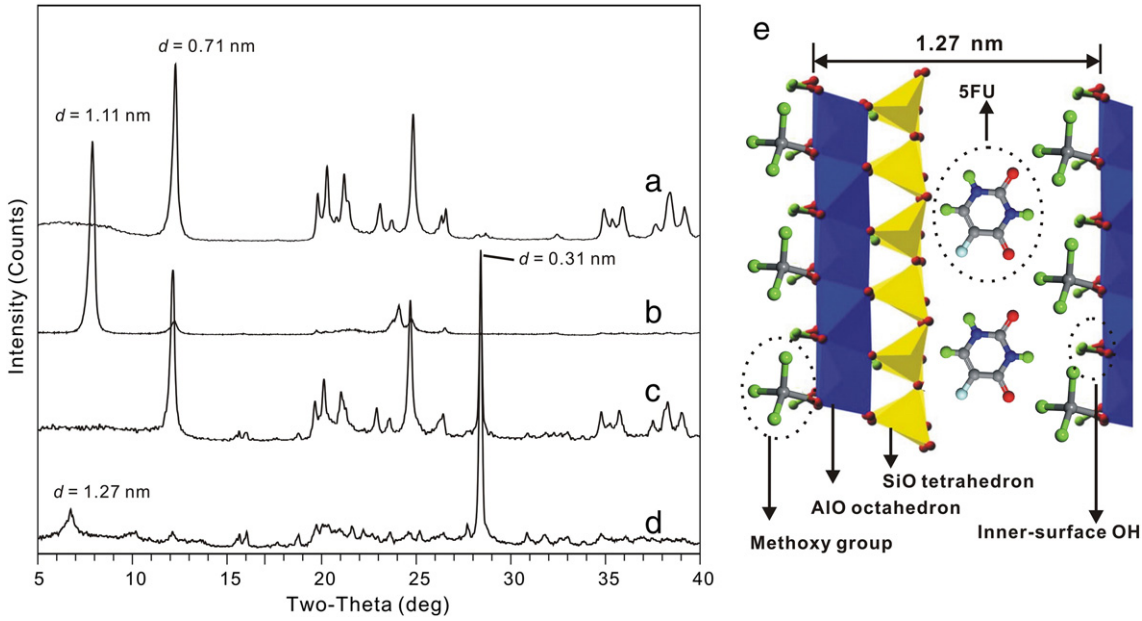

Fig. 1. XRD patterns of: (a) kaolinite, (b) Kaol-MeOH, (c) 5FU-Kaol, and (d) 5FU-Kaol-MeOH; and (e) the schematic illustration of 5FU intercalated kaolinite.

state. Therefore, the reflection at 0.31 nm represents the 5FU crystallites loaded on the external surface of kaolinite. The intensity of the reflection at 0.31 nm in 5FU-Kaol-MeOH is higher than that in 5FU-Kaol, indicating a greater surface loading of 5FU in 5FU-Kaol-MeOH. A possible reason is that the AlOH groups, on the external basal surface, on the exposed broken edges sites, and on the crystallographic defects sites of kaolinite, were grafted by methoxy groups; and this methoxy-modification enhancing the affinity between 5FU and the external surface of kaolinite permitted more 5FU to be loaded on the surface of the modified kaolinite.

The kaolinite particles have a typical pseudo-hexagonal morphology (Fig. 2a). The methoxy modification did not change the platy morphology of the initial kaolinite (related microscopic images not shown). In the TEM images of 5FU-Kaol (Fig. 2b) and 5FU-Kaol-MeOH (Fig. 2c), the aggregation of 5FU crystallite particles on the external surface of kaolinite particles was observed. The loading of 5FU aggregates resulted in the blurring of the original pseudo-hexagonal morphology of kaolinite, and the edges of kaolinite particles became poorly resolved (as denoted by the dots in the boxes in Fig. 2b and c). The aggregation of 5FU on the external surface of kaolinite may be caused by hydrogen bonds and/or van der Waals forces between the siloxane groups of kaolinite and 5FU molecules.

The 5FU-loading content, calculated from the elemental analysis, was 55.4 mass% for 5FU-Kaol-MeOH. This value is much higher than 5FU-Kaol (22.4 mass%), suggesting that the methoxy-modification substantially promoted the loading of 5FU on kaolinite in agreement with the XRD result, which showed that methoxy modification of kaolinite permitted the intercalation of 5FU into the interlayer space of kaolinite and that more 5FU was loaded onto the external surface of kaolinite.

3.2. DRIFT spectroscopy and thermal analysis

In the DRIFT spectrum of kaolinite (Fig. 3a), the vibrations at 3696, 3669, and 3653 cm^{-1} are ascribed to the O–H stretching of inner-surface hydroxyl (AlOH) groups of kaolinite, and the vibration at 3621 cm^{-1} is attributed to the O–H stretching of inner hydroxyl groups (Madejova and Komadel, 2001). In the DRIFT spectrum of Kaol-MeOH (Fig. 3b), the intensities of the three inner-surface hydroxyl groups were weakened, which was due to the consumption of inner-surface AlOH groups during methoxy modification that one MeOH molecule condensed with one AlOH group to form Al–O–C bonding and one H_2O molecule (Tunney and Detellier, 1996). The vibrations at 3022 and 2936 cm^{-1}, as well as 2848 cm^{-1}, which are ascribed to C–H stretching, also confirmed the grafting of methoxy groups. The 3550 cm^{-1} band is characteristic of hydrated kaolinite (Tunney and Detellier, 1994), which indicates that hydrogen bonds between AlOH groups and interlayer water molecules were present.

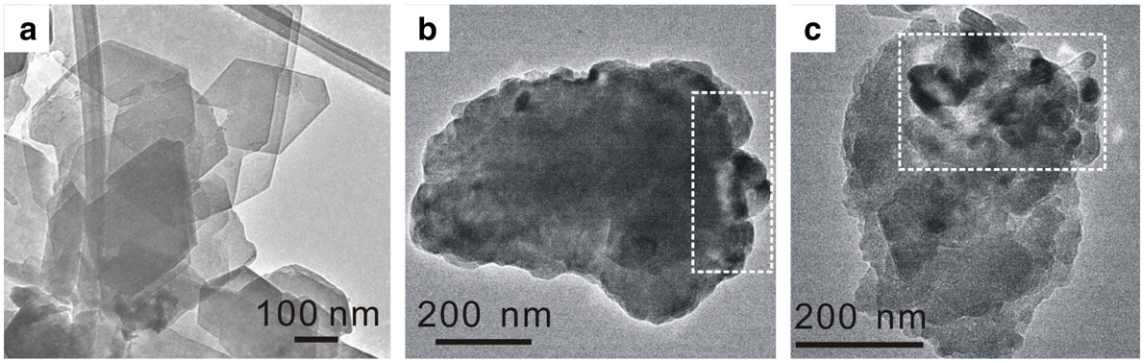

Fig. 2. TEM images of (a) kaolinite, (b) 5FU-Kaol, and (c) 5FU-Kaol-MeOH.

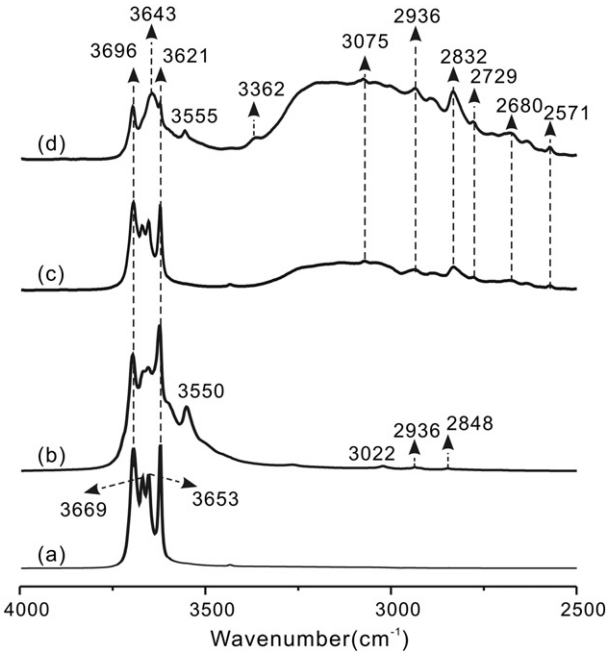

Fig. 3. DRIFT spectra of (a) kaolinite, (b) Kaol-MeOH, (c) 5FU-Kaol, and (d) 5FU-Kaol-MeOH.

In the spectra of 5FU-loaded kaolinite samples (Fig. 3c and d), several observed typical vibrations of 5FU, including 3075, 2936, 2832, 2729, 2680, and 2571 cm^{-1}, suggested the loading of 5FU on kaolinite. The intensities of the 5FU vibrations were stronger in the DRIFT spectrum of 5FU-Kaol-MeOH than 5FU-Kaol; this result was due to the higher loading of 5FU in 5FU-Kaol-MeOH. The N – H stretching vibration in pure 5FU is at 3122 cm^{-1} (Bayomi and Al-Badr, 1990). In the case of 5FU-loaded kaolinite, the N – H stretching vibration showed a redshift to 3075 cm^{-1}. This shift was due to the formation of hydrogen bonds between 5FU molecules. The loading mechanism of 5FU on the external surface of kaolinite was as follows: first, the 5FU molecules were anchored by hydrogen bonding on the external siloxane groups of kaolinite (Aguzzi et al., 2007); then, other 5FU molecules in solution were further bound to the anchored 5FU by hydrogen bonding to form hydrogen-bonded aggregates, such as dimers and trimers (Hamad et al., 2006).

For 5FU-Kaol, the vibrations of the inner-surface hydroxyl groups and the inner hydroxyl groups were almost unchanged during the 5FU loading (Fig. 3c). This result occurred because 5FU did not intercalate into the interlayer space of kaolinite. For 5FU-Kaol-MeOH, the vibration band at 3555 cm^{-1} is ascribed to the hydrogen bonds between the intercalated 5FU molecules and the inner-surface AlOH groups. The vibration band at 3362 cm^{-1}, which only appeared in 5FU-Kaol-MeOH, is ascribed to the N – H stretching vibration of the cyclic imide (CO – NH – CO). Rastogi et al. (2000) used density functional theory methods to calculate the N – H stretching vibration of the cyclic imide (CO – NH – CO) at 3479 cm^{-1}. The redshift in N – H stretching suggests that hydrogen bonds were generated between the cyclic imide (CO – NH – CO) of the intercalated 5FU and the AlOH groups of kaolinite. It is noteworthy that in 5FU-Kaol-MeOH the original O – H stretching bands at 3669 and 3653 cm^{-1} overlapped and shifted to lower frequency at 3643 cm^{-1}. This shift is caused by the disturbance of the hydrogen bonds between 5FU and the inner-surface AlOH groups.

In the TG curve of kaolinite (Fig. 4a), the major mass loss at approximately 400 to 600 °C is attributed to dehydroxylation of the structural AlOH groups, which corresponds to the endothermic peaks at 507.8 °C in the DSC curve. This result is in agreement with the observation that the dehydroxylation of kaolinite occurs at approximately 400 to 600 °C (Kristof et al., 2002). Two mass losses are observed in the TG curve of Kaol-MeOH (Fig. 4b). Because the methoxy groups are stable up to 350 °C, the first slow loss at approximately 100 to 300 °C is attributed to the dehydration of the physically adsorbed water and the interlayer water generated by the condensation between MeOH molecules and AlOH groups of kaolinite (Komori et al., 2000; Tunney and Detellier, 1996). The second substantial loss at approximately 300 to 600 °C represents the decomposition of the grafted methoxy groups and the dehydroxylation of kaolinite.

In the TG curve of 5FU-Kaol (Fig. 4c), two steps with noticeable mass loss are clearly resolved. The first step in the range of 250 to 350 °C is attributed to the decomposition of 5FU loaded on the external surface of kaolinite, corresponding to the endothermic peak at 320.4 °C in the DSC curve. The second step from 400 to 600 °C is due to the dehydroxylation of kaolinite, corresponding to the endothermic peak at 528.5 °C. This value is higher than pure kaolinite (507.8 °C), which may be caused by the incomplete thermal decomposition of 5FU. The endothermic peak at 282.2 °C in the DSC curve is attributed to the melting of 5FU crystallites.

In the TG curve of 5FU-Kaol-MeOH (Fig. 4d), the first rapid mass loss from 250 to 420 °C is ascribed to two thermal episodes: (i) the loss of methoxy groups, which only makes a minor contribution to the total mass loss; (ii) the decomposition of the surface-loaded 5FU and the interlayer-loaded 5FU, which makes the dominant contribution to the mass loss. The two endothermic peaks at 285.3 and 338.3 °C in the DSC curve are attributed to the melting of 5FU crystallites and the decomposition of 5FU, respectively. The value of the decomposition temperature of 5FU in the DSC curve of 5FU-Kaol-MeOH (338.3 °C) is higher than that in 5FU-Kaol (320.4 °C), and the range of decomposition of 5FU in 5FU-Kaol-MeOH (250–420 °C) is broader than that in 5FU-Kaol (250–350 °C), indicating that the intercalated 5FU is more thermally stable than the surface-loaded 5FU. This is in agreement with a higher thermal stability of other intercalated organic guests which decomposed at higher temperatures in the interlayer space of clay minerals, such as cationic surfactant in montmorillonite (He et al., 2005), organosilane in silane-grafted kaolinite (Yang et al., 2012), and 5FU in layered double hydroxides (Wang et al., 2005). The mass loss of AlOH in the TG curve of 5FU-Kaol-MeOH, from 400 to 600 °C, was not as clear as that in the three other kaolinite, Kaol-MeOH, and 5FU-Kaol samples. This difference may be caused by two factors: (i) the high loading of 5FU (55.4 mass%) in 5FU-Kaol-MeOH, which creates a lower kaolinite concentration than in the other three kaolinite samples; and (ii) the overlap between the decomposition of the AlOH groups of kaolinite and the decomposition of the residual intercalated and surface-loaded 5FU.

Because the amorphous 5FU in the interlayer space of kaolinite was not endothermic during the melting phase, the endothermic peak at approximately 280 °C represents the melting of 5FU crystallites loaded on the external surface of kaolinite. The area of this endothermic peak corresponds to the heat of fusion of 5FU crystallites. The area is directly proportional to the heat absorbed during the melting and to the mass of the test sample (Coleman and Craig, 1996). The peak area (A) is related to the enthalpy change by the following relationship:

$$A = k' m(-\Delta H)$$

where k' is a calorimetric sensitivity, m is the mass of the sample, and $-\Delta H$ is the enthalpy change. According to this calculation, the area of the endothermic peak of melting of 5FU is 28.1 J/g in 5FU-Kaol and 51.2 J/g in 5FU-Kaol-MeOH, respectively. Because of the similar crystallization condition and crystallite sizes of 5FU in modified and unmodified kaolinite, 5FU crystallites in 5FU-Kaol and 5FU-Kaol-MeOH theoretically had identical heat of fusion (A) and enthalpy change ($-\Delta H$) under the same temperature and pressure. Therefore, the unequal values of A for 5FU-Kaol and 5FU-Kaol-MeOH were directly related to the different mass of the 5FU crystallites (m). As a result, the amount of the 5FU crystallites (the surface-loaded

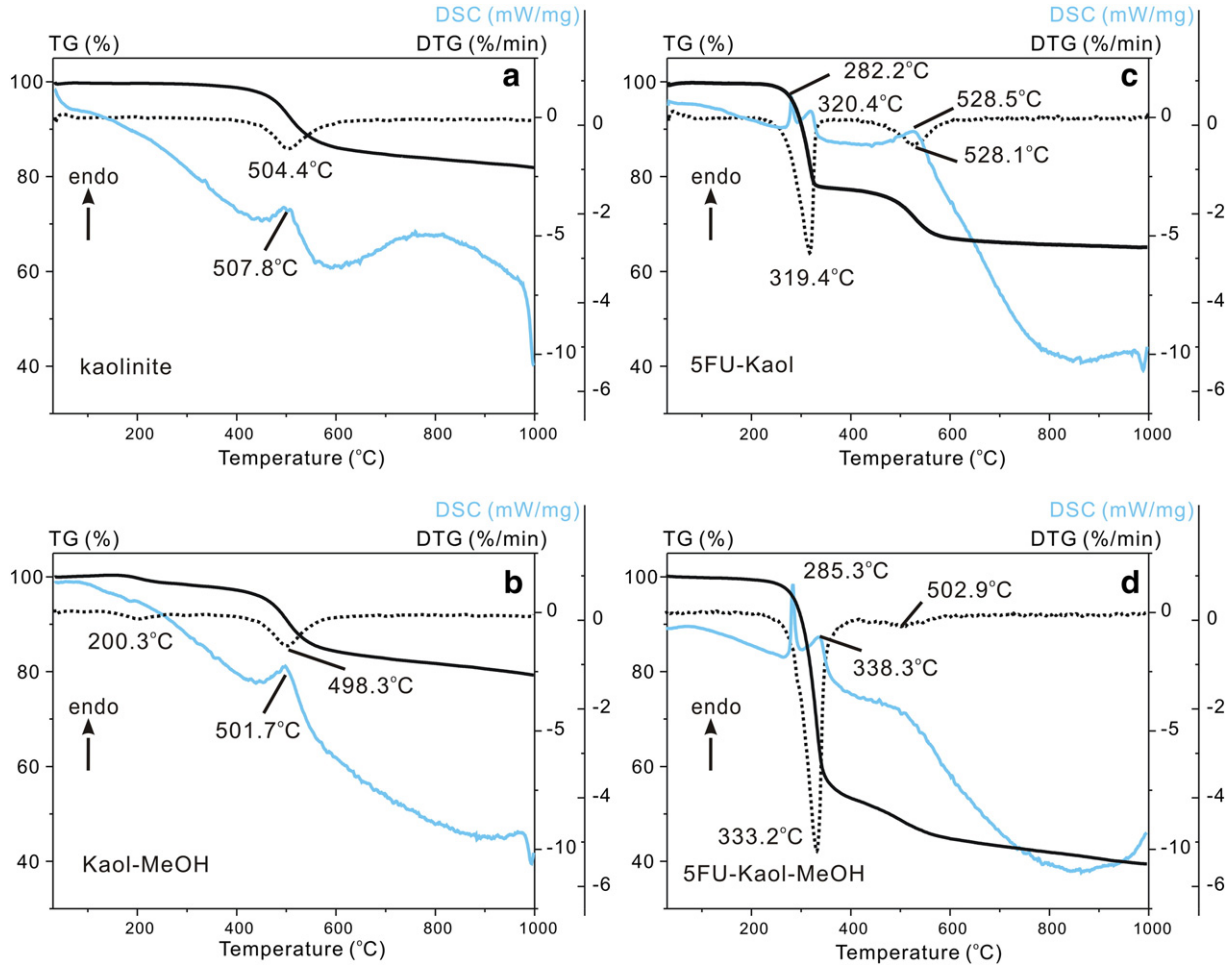

Fig. 4. TG, DTG, and DSC curves of (a) kaolinite, (b) Kaol-MeOH, (c) 5FU-Kaol, and (d) 5FU-Kaol-MeOH.

5FU) in 5FU-Kaol-MeOH was found to be 1.82 times larger than that in 5FU-Kaol (22.4 mass%). Thus, the 5FU-loading content for the interlayer-loaded 5FU and the surface-loaded 5FU was 14.6 mass% and 40.8 mass%, respectively. The lower loading of interlayer-loaded 5FU may be because that the interlayer space of the kaolinite was much more limited than the external surface space. It is noteworthy that the accuracy of the calculated area of the endothermic peak of melting was limited by the lack of definition of a true baseline across the peak region (Coleman and Craig, 1996). The amount of 5FU for the surface-loaded and interlayer-loaded 5FU may deviate from the actual value.

The loading capacity of 5FU (55.4 mass%) on the methoxy-modified kaolinite was larger than that on montmorillonite (approximately 45 mass%) (Lin et al., 2002), layered double hydroxides (approximately 40 mass%) (Wang et al., 2005), and zeolites (approximately 10 mass%) (Datt et al., 2013). The high-capacity loading of 5FU on the methoxy-modified kaolinite is attributed to the dual-functions of methoxy modification: (i) methoxy modification causes 5FU intercalation into the interlayer space of kaolinite, which is achieved by displacement of the interlayer MeOH molecules; and (ii) methoxy modification increases the loading of 5FU on the external surface of kaolinite, which is achieved by enhancing the affinity between 5FU and the methoxy-modified kaolinite.

In consideration of that many drugs and even some agrochemicals have similar functional groups and molecular dimensions to 5FU, one can anticipate that these guest molecules should intercalate into the interlayer space and load onto the external surface of the methoxy-modified kaolinite through a similar loading mechanism as 5FU on the methoxy-modified kaolinite. Based on these results, the methoxy-modified kaolinite should be a very promising carrier material in pharmaceutics, particularly in the agrochemical industry, for three reasons: (i) the guests had a high-capacity loading on the methoxy-modified kaolinite, (ii) the intercalated guests in the interlayer space of the methoxy-modified kaolinite showed a high thermal and/or chemical stability because of the protection of the lamellar structure of the kaolinite, and (iii) the intercalated guests may have the potential for controlled release due to the diffusion of guest molecules from the confined interlayer space of the methoxy-modified kaolinite.

4. Conclusions

Kaolinite was used as a drug carrier for the loading of 5FU. 5FU was loaded in crystallite form on the external surface of kaolinite. The surface-loaded 5FU aggregated through hydrogen bonding.

Methoxy modification of kaolinite substantially promoted the loading of 5FU through both intercalation of 5FU in the interlayer space and enhancement of the loading of 5FU on the external surface of the methoxy-modified kaolinite. In the former case, 5FU was intercalated as a vertical monolayer into the interlayer space of the methoxy-modified kaolinite, and the interlayer-loaded 5FU was of higher thermal stability than the surface-loaded kaolinite. In the latter case, more 5FU, approximately twice the loading capacity of the unmodified kaolinite, was loaded on the external surface of the methoxy-modified kaolinite because of the greater affinity between 5FU and the methoxy-

modified kaolinite. This work demonstrates that methoxy-modified kaolinite is a promising drug carrier and deserves more research attentions in the field of pharmaceutics.

Acknowledgments

Financial support from the Team Project of the Natural Science Foundation of Guangdong Province, China (S2013030014241) and the National Natural Science Foundation of China (Grant No. 41072032) are gratefully acknowledged. This is a contribution (No. IS-1827) from GIGCAS.

References

Aguzzi, C., Cerezo, P., Viseras, C., Caramella, C., 2007. Use of clays as drug delivery systems: possibilities and limitations. Appl. Clay Sci. 36, 22–36.
Akalin, E., Akyuz, S., Akyuz, T., 2007. Adsorption and interaction of 5-fluorouracil with montmorillonite and saponite by FT-IR spectroscopy. J. Mol. Struct. 834–836, 477–481.
Bayomi, S.M., Al-Badr, A.A., 1990. Analytical profile of 5-fluorouracil. In: Klaus, F., Al-Bardr, A.A., Lee, T.G. (Eds.), Analytical Profiles of Drug Substances, 18. Academic Press, pp. 599–639.
Bonina, F.P., Giannossi, M.L., Medici, L., Puglia, C., Summa, V., Tateo, F., 2007. Adsorption of salicylic acid on bentonite and kaolin and release experiments. Appl. Clay Sci. 36, 77–85.
Burton, A.W., Ong, K., Rea, T., Chan, I.Y., 2009. On the estimation of average crystallite size of zeolites from the Scherrer equation: a critical evaluation of its application to zeolites with one-dimensional pore systems. Microporous Mesoporous Mater. 117, 75–90.
Carretero, M.I., 2002. Clay minerals and their beneficial effects upon human health. A review. Appl. Clay Sci. 21, 155–163.
Carretero, M.I., Pozo, M., 2009. Clay and non-clay minerals in the pharmaceutical industry: part I. Excipients and medical applications. Appl. Clay Sci. 46, 73–80.
Carretero, M.I., Pozo, M., 2010. Clay and non-clay minerals in the pharmaceutical and cosmetic industries. Part II. Active ingredients. Appl. Clay Sci. 47, 171–181.
Castellano, M., Turturro, A., Riani, P., Montanari, T., Finocchio, E., Ramis, G., Busca, G., 2010. Bulk and surface properties of commercial kaolins. Appl. Clay Sci. 48, 446–454.
Choy, J.H., Choi, S.J., Oh, J.M., Park, T., 2007. Clay minerals and layered double hydroxides for novel biological applications. Appl. Clay Sci. 36, 122–132.
Coleman, N.J., Craig, D.Q.M., 1996. Modulated temperature differential scanning calorimetry: a novel approach to pharmaceutical thermal analysis. Int. J. Pharm. 135, 13–29.
Datt, A., Burns, E.A., Dhuna, N.A., Larsen, S.C., 2013. Loading and release of 5-fluorouracil from HY zeolites with varying SiO_2/Al_2O_3 ratios. Microporous Mesoporous Mater. 167, 182–187.
Frost, R.L., Tran, T.H., Kristof, J., 1997. The structure of an intercalated ordered kaolinite: a Raman microscopy study. Clay Miner. 32, 587–596.
Frost, R.L., Kristof, J., Paroz, G.N., Kloprogge, J.T., 1998. Role of water in the intercalation of kaolinite with hydrazine. J. Colloid Interface Sci. 208, 216–225.
Frost, R.L., Kristof, J., Horvath, E., Kloprogge, J.T., 2000. Effect of water on the formamide-intercalation of kaolinite. Spectrochim. Acta A Mol. Biomol. Spectrosc. 56, 1711–1729.
Hamad, S., Moon, C., Catlow, C.R.A., 2006. Kinetic insights into the role of the solvent in the polymorphism of 5-fluorouracil from molecular dynamics simulations. J. Phys. Chem. B 110, 3323–3329.
He, H.P., Ding, Z., Zhu, J.X., Yuan, P., Xi, Y.F., Yang, D., Frost, R.L., 2005. Thermal characterization of surfactant-modified montmorillonites. Clay Clay Miner. 53, 287–293.
Komori, Y., Matsumura, A., Itagaki, T., Sugahara, Y., Kuroda, K., 1999a. Preparation of a kaolinite-ε-caprolactam intercalation compound. Clay Sci. 11, 47–55.
Komori, Y., Sugahara, Y., Kuroda, K., 1999b. Direct intercalation of poly(vinylpyrrolidone) into kaolinite by a refined guest displacement method. Chem. Mater. 11, 3–6.
Komori, Y., Sugahara, Y., Kuroda, K., 1999c. Intercalation of alkylamines and water into kaolinite with methanol kaolinite as an intermediate. Appl. Clay Sci. 15, 241–252.
Komori, Y., Enoto, H., Takenawa, R., Hayashi, S., Sugahara, Y., Kuroda, K., 2000. Modification of the interlayer surface of kaolinite with methoxy groups. Langmuir 16, 5506–5508.
Kristof, J., Frost, R.L., Kloprogge, L.T., Horvath, E., Mako, E., 2002. Detection of four different OH-groups in ground kaolinite with controlled-rate thermal analysis. J. Therm. Anal. Calorim. 69, 77–83.
Kuroda, K., Hiraguri, K., Komori, Y., Sugahara, Y., Mouri, H., Uesu, Y., 1999. An acentric arrangement of *p*-nitroaniline molecules between the layers of kaolinite. Chem. Commun. 2253–2254.
Kuroda, Y., Ito, K., Itabashi, K., Kuroda, K., 2011. One-step exfoliation of kaolinites and their transformation into nanoscrolls. Langmuir 27, 2028–2035.
Lagaly, G., Ogawa, M., Dekany, M., 2006. Clay mineral organic interactions. In: Bergaya, F., Theng, B.K.G., Lagaly, G. (Eds.), Handbook of Clay Science. Elsevier, Amsterdam, pp. 309–377.
Lin, F.H., Lee, Y.H., Jian, C.H., Wong, J.M., Shieh, M.J., Wang, C.Y., 2002. A study of purified montmorillonite intercalated with 5-fluorouracil as drug carrier. Biomaterials 23, 1981–1987.
Lvov, Y.M., Shchukin, D.G., Mohwald, H., Price, R.R., 2008. Halloysite clay nanotubes for controlled release of protective agents. ACS Nano 2, 814–820.
Ma, C., Eggleton, R.A., 1999. Cation exchange capacity of kaolinite. Clay Clay Miner. 47, 174–180.
Madejova, J., Komadel, P., 2001. Baseline studies of the clay minerals society source clays: infrared methods. Clay Clay Miner. 49, 410–432.
Mallick, S., Pattnaik, S., Swain, K., De, P.K., Saha, A., Ghoshal, G., Mondal, A., 2008. Formation of physically stable amorphous phase of ibuprofen by solid state milling with kaolin. Eur. J. Pharm. Biopharm. 68, 346–351.
Matsumura, A., Komori, Y., Itagaki, T., Sugahara, Y., Kuroda, K., 2001. Preparation of a kaolinite-nylon 6 intercalation compound. Bull. Chem. Soc. Jpn. 74, 1153–1158.
McCarron, P.A., Woolfson, A.D., Keating, S.M., 2000. Sustained release of 5-fluorouracil from polymeric nanoparticles. J. Pharm. Pharmacol. 52, 1451–1459.
Niwa, T., Takeuchi, H., Hino, T., Kunou, N., Kawashima, Y., 1993. Preparations of biodegradable nanospheres of water-soluble and insoluble drugs with D,L-lactide glycolide copolymer by a novel spontaneous emulsification solvent diffusion method, and the drug release behavior. J. Control. Release 25, 89–98.
Price, R.R., Gaber, B.P., Lvov, Y., 2001. In-vitro release characteristics of tetracycline HCl, khellin and nicotinamide adenine dineculeotide from halloysite; a cylindrical mineral. J. Microencapsul. 18, 713–722.
Rastogi, V.K., Jain, V., Yadav, R.A., Singh, C., Palafox, M.A., 2000. Fourier transform Raman spectrum and *ab initio* and density functional computations of the vibrational spectrum, molecular geometry, atomic charges and some molecular properties of the anticarcinogenic drug 5-fluorouracil. J. Raman Spectrosc. 31, 595–603.
Sliwinska-Bartkowiak, M., Dudziak, G., Gras, R., Sikorski, R., Radhakrishnan, R., Gubbins, K.E., 2001. Freezing behavior in porous glasses and MCM-41. Colloids Surf. A Physicochem. Eng. Asp. 187, 523–529.
Takenawa, R., Komori, Y., Hayashi, S., Kawamata, J., Kuroda, K., 2001. Intercalation of nitroanilines into kaolinite and second harmonic generation. Chem. Mater. 13, 3741–3746.
Tan, D.Y., Yuan, P., Annabi-Bergaya, F., Yu, H.G., Liu, D., Liu, H.M., He, H.P., 2013. Natural halloysite nanotubes as mesoporous carriers for the loading of ibuprofen. Microporous Mesoporous Mater. 179, 89–98.
Tunney, J., Detellier, C., 1994. Preparation and characterization of an 8.4-Angstrom hydrate of kaolinite. Clay Clay Miner. 42, 473–476.
Tunney, J., Detellier, C., 1996. Chemically modified kaolinite. Grafting of methoxy groups on the interlamellar aluminol surface of kaolinite. J. Mater. Chem. 6, 1679–1685.
Wang, Z.L., Wang, E.B., Gao, L., Xu, L., 2005. Synthesis and properties of Mg_2Al layered double hydroxides containing 5-fluorouracil. J. Solid State Chem. 178, 736–741.
Yang, S.Q., Yuan, P., He, H.P., Qin, Z.H., Zhou, Q., Zhu, J.X., Liu, D., 2012. Effect of reaction temperature on grafting of γ-aminopropyl triethoxysilane (APTES) onto kaolinite. Appl. Clay Sci. 62–63, 8–14.
Yuan, P., Southon, P.D., Liu, Z.W., Green, M.E.R., Hook, J.M., Antill, S.J., Kepert, C.J., 2008. Functionalization of halloysite clay nanotubes by grafting with γ-aminopropyltriethoxysilane. J. Phys. Chem. C 112, 15742–15751.
Yuan, P., Southon, P.D., Liu, Z.W., Kepert, C.J., 2012. Organosilane functionalization of halloysite nanotubes for enhanced loading and controlled release. Nanotechnology 23, 375705.
Zeng, Q.H., Yu, A.B., Lu, G.Q., Standish, R.K., 2003. Molecular dynamics simulation of organic–inorganic nanocomposites: layering behavior and interlayer structure of organoclays. Chem. Mater. 15, 4732–4738.